Supporting Information

Rational design for the separation of metallic and semiconducting single-walled carbon nanotubes by magnetic field

Chengzhi Luo [a], Da Wan [a], Junji Jia [b, a], Delong Li [a], Chunxu Pan [a, c*], Lei Liao [a*]

a School of Physics and Technology, and MOE Key Laboratory of Artificial Micro- and Nano-structures, Wuhan University, Wuhan 430072, China.

b Center for Theoretical Physics, Wuhan University, Wuhan 430072, China.

c Center for Electron Microscopy, Wuhan University, Wuhan 430072, China.

*Author to whom correspondence should be addressed.
E-mail: cxpan@whu.edu.cn (C. Pan), liaolei@whu.edu.cn (L. Liao);

Tel: +86-27-68752481 ext. 8168;

Supporting Information 1: Supporting Figure

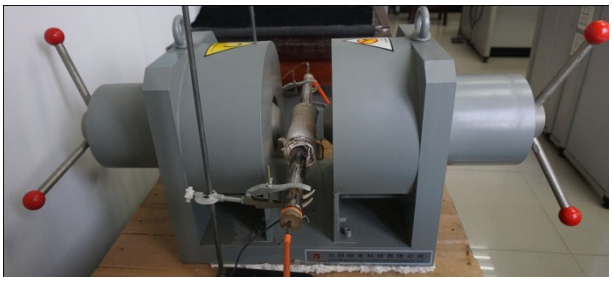

Figure S1. The experimental setup for preparing s-SWNTs within a magnetic field.

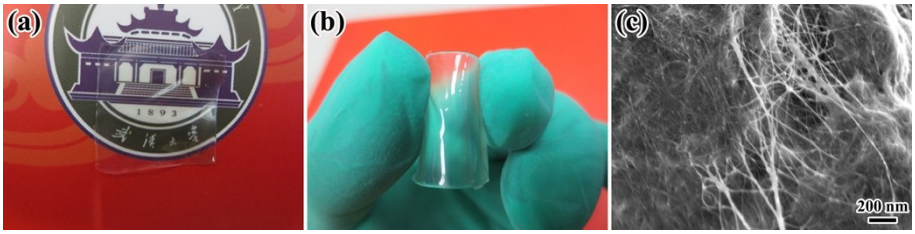

Figure S2. Direct deposition of the SWNTs on a polymethyl methacrylate (PMMA) substrate of 2 × 2 cm under 1 T magnetic field assistance. (a, b) Optical image (c) SEM morphology.

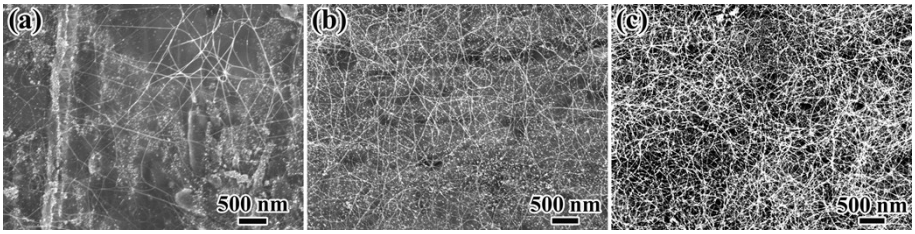

Figure S3. SEM morphologies of the SWNTs with different preparation durations. (a) 5 min, (b) 15 min, (c) 30 min. Obviously, the density of the SWNTs can be controlled by deposition times, i.e. the longer the deposition time, the higher the density of the SWNTs.

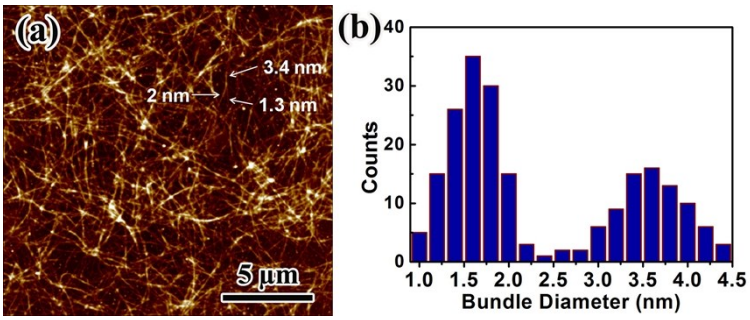

Figure S4. (a) AFM image of the SWNT network on the Si substrate, and (b) diameter distribution of the SWNT bundles.

Obviously, the diameters are largely centered in the ranges of 1.0 - 2.4 nm and 3.0 - 4.5 nm. The diameters within 1.0-2.4 nm are almost equal to the diameter of individual SWNTs, while the diameter within 3.0-4.5 nm is referred to the SWNT bundles. Therefore, the Y-junction network of the present samples is considered to mainly consist of individual nanotubes, whereas bundles of a few nanotubes exist at some parts.

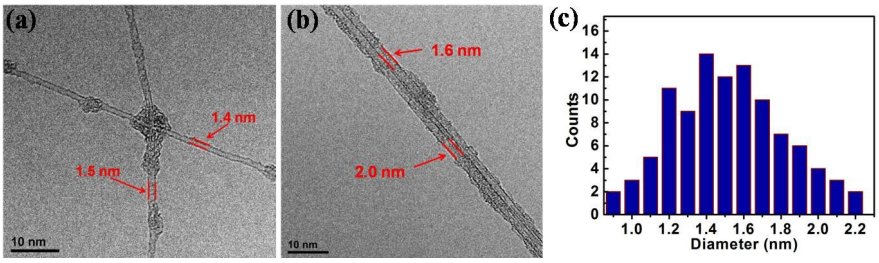

Figure S5. (a) (b) Typical HRTEM images of the SWNTs. (c) Diameter distribution of the 100 SWNTs from 30 HRTEM images.

HRTEM is powerful tool to directly observe the SWNTs microstructures. We can accurately measure the diameter of the SWNTs from the HRTEM images. We randomly measured the diameter of 100 SWNTs from 30 HRTEM images and got the statistical value. The diameter distribution is about 0.9-2.2 nm, which further confirmed the AFM results.

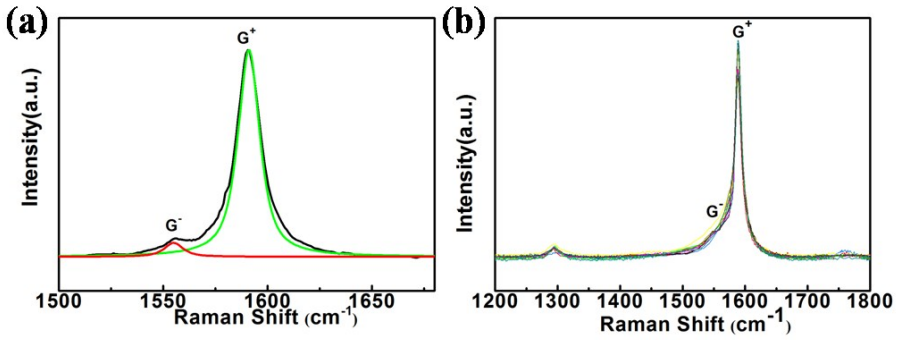

Figure S6. G-bands of Raman spectra of the 1 T-SWNTs. (a) Typical G-band fitted by G+ and G- peaks. (b) G-bands that obtained using 633 nm excitation laser at 10 different spots over the substrate. Each curve shows spectrum at a spot on the substrate.

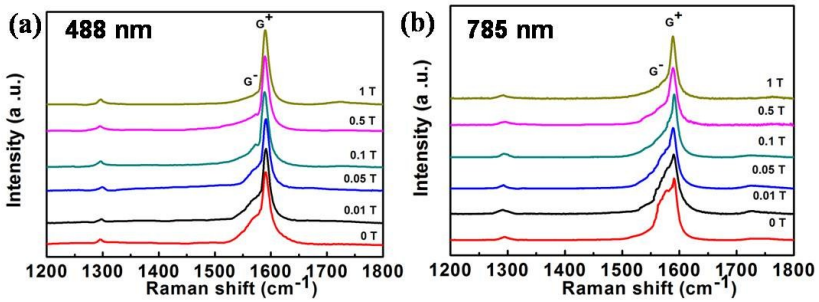

Figure S7. Typical G-bands of Raman spectra of the samples 0 T-, 0.01 T-, 0.05 T-, 0.1 T-, 0.5 T- and 1 T-SWNTs using the excitation laser wavelengths of (a) 488 nm and (b) 785 nm.

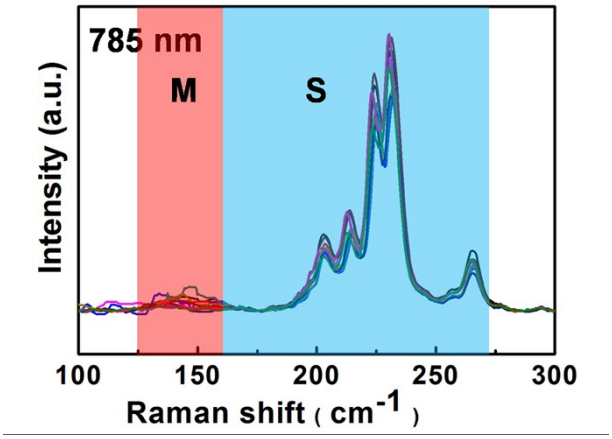

Figure S8. Raman spectra of the sample 1 T-SWNTs at 1.58 eV (785 nm) excitation, which are measured at over 10 different locations. The pink shaded region represents transitions resonant with 1.58 eV for the metallic SWNTs, while the blue shaded region is for the semiconducting SWNTs.

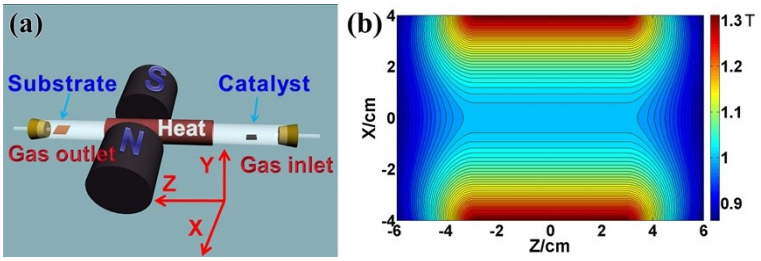

Figure S9. Theoretical simulation of the magnetic field that created by the two poles of electromagnet. (a) Schematic diagram of the magnetic field-assisted FC-CVD reactor in the present work. X-axis is perpendicular to electromagnet, Z-axis is along the gas flow direction, and Y-axis is perpendicular to X and Z-axis. (b) Simulation of the magnetic field in the X-Z plane. The strength of central magnetic field is 1 T. The paramagnetic or ferromagnetic particle is always attracted to regions of the highest magnetic field strength, i.e. close to the magnet, while the diamagnetic particle is always repelled to regions of lowest magnetic field strength, i.e. far away from the magnet in the present case.

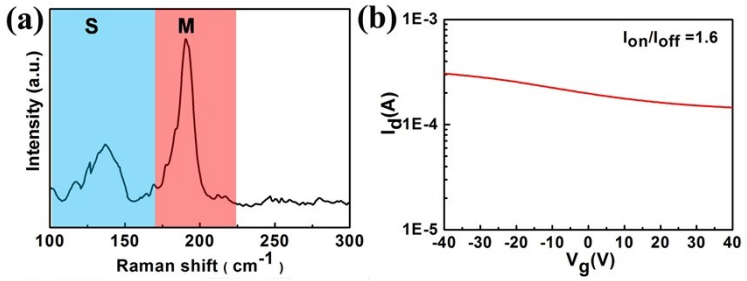

Figure S10. Characterizations of the SWNTs that were collected from the wall of the quartz tube. (a) Raman spectra at 1.96 eV (633 nm) excitation. The pink shaded region represents the transitions resonant with 1.96 eV for metallic SWNTs, while the blue shaded region is for the semiconducting SWNTs. The metallic peak is stronger than the semiconducting peak. (b) Typical transport property of the SWNT-based TFT. The bias voltage V_{ds} is maintained at 1 V. The calculated I_{on}/I_{off} is 1.6. Obviously, the characterizations from both Raman spectra and transport property indicate that the sample was mainly composed of the metallic SWNTs.

Supporting Information 2: Theory and Modeling

Since the SWNTs are commonly described as high aspect ratio rodlike particles,[1, 2] we consider SWNTs to behave like a dipole. We examine a dilute dispersion of noninteracting SWNTs, which enables us to consider the motion of each nanotube independently and determine the bulk distribution by summing the contributions from each nanotube. As we illustrated in the main text, the motion of s-SWNTs was along the direction of gas flow without direction change and m-SWNTs would change the flowing direction and deposited on the wall of quartz tube. Therefore, we only need to consider the effect of magnetic field to m-SWNTs. In our model, the X-axis is perpendicular to electromagnet, Z-axis is along the gas flow direction and Y-axis is perpendicular to X and Z-axis, as shown in Figure S6a.

Unlike in previous publications,[2-4] the SWNTs in our approach could be thought as dispersed in Ar/H_2 gas, which has a much lower viscosity coefficient (~1×10^{-5} Pa s) than that of a liquid medium (such as epoxy resin, 0.90-0.95 Pa s).[3] The utra-low medium viscosity, such as in Ar/H_2 gas, will lead to an ultra-low viscous force. Therefore, for simplicity's sake, we ignore the influence of the viscous force on SWNTs.

When a m-SWNT is placed in the inhomogeneous magnetic field, the force along the X-axis on a single m-SWNT is then[5]

$$F_x = m_{\mu x}\frac{dB}{dx} \quad (1)$$

where $m_{\mu x}$ is the magnetic moment of m-SWNT, $\frac{dB}{dx}$ is the magnetic field gradient in the X-axis. When a magnetic force is applied, a single m-SWNT will accelerate in the direction of that force. The acceleration is

$$a_x = \frac{F_x}{m} \quad (2)$$

where m is the mass of m-SWNT. We can get the velocity in the X-axis

$$v_x = a_x t + v_{x0} \quad (3)$$

where t is the time of flight, v_{x0} is velocity in the X-axis before entering the magnetic field. In our experiment, the gas flow rate is constant (v_g) which equals to the velocity of m-SWNT in the Z-axis. The flight time could be calculated as

$$t = \frac{L}{v_g} \quad (4)$$

where L is the distance between reaction zone and the substrate. Then, the distance a SWNT travelled in X-axis is

$$d_x = \frac{1}{2}(v_x + v_{x0})t \tag{5}$$

Because of the m-SWNT has different initial position (x_0), the final position of the m-SWNT in the X-axis is

$$x = x_0 + d_x \tag{6}$$

Combine Eq. (1) - (6) and solving for x, we get

$$x = x_0 + \frac{1}{2}\left(\frac{m_{\mu x}\frac{dB}{dx}L}{mv_{z0}^2} + 2\frac{v_{x0}}{v_{z0}}\right)L \tag{7}$$

Furthermore, we approximate the velocity distribution of nanotubes at temperature T before entering the magnetic field B by the Maxwell-Boltzmann distribution function

$$f(v_0) = \frac{1}{4}\sqrt{2}\left(\frac{m}{\pi k_b T}\right)^{3/2} e^{-\frac{1}{2}\frac{m[v_{x_0}^2 + v_{y_0}^2 + (v_{z_0} - v_g)^2]}{k_b T}} \tag{8}$$

where k_b is Boltzmann's constant, v_{x0}, v_{y0}, and v_{z0} is the velocity in the X-, Y-, and Z-axis, respectively. Using this velocity distribution function and relation (7), one can derive the spatial probability distribution function in the X-direction

$$g(x) = f(v_0)\frac{dv_{x0}}{dx} \tag{9}$$

Combine Eq. (4), (5), (8) and (9), we get

$$g(x) = \frac{1}{4}\sqrt{2}\left(\frac{m}{\pi k_b T}\right)^{3/2} e^{-\frac{1}{2}\frac{m[v_{x_0}^2 + v_{y_0}^2 + (v_{z_0} - v_g)^2]}{k_b T}}\frac{v_g}{L} \tag{10}$$

Here we only consider the velocity in the X-axis. After integrating over Y and Z directions, we obtain a distribution in X-direction only

$$g'(x) = \int_{-\infty}^{+\infty}\int\frac{1}{4}\sqrt{2}\left(\frac{m}{\pi k_b T}\right)^{\frac{3}{2}} e^{-\frac{1}{2}\frac{m[v_{x_0}^2 + v_{y_0}^2 + (v_{z_0} - v_g)^2]}{k_b T}}\frac{v_g}{L}dv_{y_0}dv_{z_0} \tag{11}$$

By placing Eq. (7) into Eq. (11), we find $g'(x)$ to be

$$g'(x) = \frac{\sqrt{2}\, e^{-\frac{1}{8}\frac{(L^2 m_{\mu x}\frac{dB}{dx} - 2mv_g^2 x + 2mv_g^2 x_0)^2}{mTk_b v_g L^2}}}{2 L\sqrt{\pi m k_b T}} mv_g \quad (12)$$

In our system, the initial position (x_0) of m-SWNTs is between –R and R, where R is the radius of quartz tube. By integrating x_0, we can get

$$g''(x) = \frac{1}{4R}\left(erf\left[\frac{\sqrt{2}(2Rmv_g^2 - L^2 m_{\mu x}\frac{dB}{dx} + 2mv_g^2 x)}{4Lv_g\sqrt{mTk_b}}\right] + erf\left[\frac{\sqrt{2}(2Rmv_g^2 + L^2 m_{\mu x}\frac{dB}{dx} - 2mv_g^2 x)}{4Lv_g\sqrt{mTk_b}}\right]\right) \quad (13)$$

$$\mathrm{erf}(u) = \frac{\pi}{\sqrt{2}}\int_0^u e^{-\eta^2} d\eta$$

where erf is the error function [ ]. Eq. (13) is the probability distribution function of m-SWNTs on the substrate. For a square substrate with the side length of a, the probability that the m-SWNTs deposit on the substrate is

$$P(B) = \int_{-a/2}^{a/2} \frac{1}{4R}\left(erf\left[\frac{\sqrt{2}\left(2Rmv_g^2 - L^2 m_{\mu x}\frac{dB}{dx} + 2mv_g^2 x\right)}{4Lv_g\sqrt{mTk_b}}\right] + erf\left[\frac{\sqrt{2}\left(2Rmv_g^2 + L^2 m_{\mu x}\frac{dB}{dx} - 2mv_g^2 x\right)}{4Lv_g\sqrt{mTk_b}}\right]\right)dx \quad (14)$$

In our system, the radius of the quartz tube (R), the distance between reaction zone and the substrate (L), the gas flow rate (v_g) and the temperature (T) are constant. For a singular m-SWNT, its mass (m) is certain. Therefore, this probability mainly depends on the magnetic moment ($m_{\mu x}$) and magnetic field gradient ($\frac{dB}{dx}$). However, a few factors that will affect the floating-deposition process, such as reflection of m-SWNT on the quartz tube wall, the continuous creation during propagation along z-axis, the non-uniform temperature distribution, etc. Due to these, the factors and coefficients in Eq. (14) will receive many corrections, which are beyond analytical calculation. Noting that Eq. (14) behaves like an exponential x^2 function. In the range of parameters in our experiment, we would like to collect all factors in to a phenomenological model that containing two parameters.

$$P(B)_{ph} = \alpha e^{-\beta\left(\frac{dB}{dx}\right)^2} \quad (15)$$

where $P(B)_{ph}$ is the probability function of m-SWNTs, dB/dx is the magnetic field gradient in X-axis, α and β are two constant that associated with the initial percentage, velocity, temperature, mass, magnetic moment, etc. However, since we do not know dB/dx but only B, we will have to replace dB/dx by some function of B. Moreover, the exact relation between dB/dx and B is unknown either but they are expected to be monotonically correlated. Therefore, we use a relation

$$\frac{dB}{dx} = \gamma B^n \tag{16}$$

where γ>0, n>0. Then the probability function becomes

$$P(B)_{ph} = \alpha e^{-\delta B^{2n}} \tag{17}$$

in which $\delta=\beta\times\gamma^2$ is the single constant that combined β and γ. The percentage of m-SWNTs, denoted as f(B), is related to $P(B)_{ph}$ by

$$f(B) = \frac{P(B)_{ph}}{1 + P(B)_{ph}} \tag{18}$$

We can now use this model to fit the percentage of m-SWNTs on the substrate. Figure 5 compares the experimental data with that obtained from our calculation as a function of applied magnetic field. Because the samples were not from the same batch for the different applied magnetic field, there was a fluctuation of the measured data when compared to the theoretical mode. Nonetheless, the theory supported the data very well in that the percentage of m-SWNTs is highly relevant to the magnetic field gradient/strength i.e. the bigger the magnetic field gradient/strength, the lower the percentage of m-SWNTs.

Furthermore, from the from the calculation of our theory, one can study the effect of many other parameters to the percentage of the m-SWNTs, such as the gas flow rate (V_g) and the distance between reaction zone and the substrate (L), etc. When the V_g is increased proportionally while the magnetic field and growth rate are unchanged, it is found that the percentage of m-SWNTs will increase accordingly. This agrees with our physical expectation that the faster V_g will allow shorter time for the m-SWNTs to move towards the region of maximal magnetic field. The L can affect the percentage of m-SWNTs in the same way. The longer L will allow longer time for the m-SWNTs to move towards the region of maximal magnetic field, which will result in lower percentage of m-SWNT. In other words, we can further enhance

the percentage of s-SWNTs by adjusting the other parameters, such as decrease the gas flow rate and prolong the distance between reaction zone and the substrate, etc.

Reference

1 R. Duggal, M. Pasquali, Phys. Rev. Lett. 2006, **96**, 246104.

2 J. Shaver, A. N. G. Parra-Vasquez, S. Hansel, O. Portugall, C. H. Mielke, M. v. Ortenberg, R. H. Hauge, M. Pasquali, J. Kono, ACS Nano 2009, **3**, 131.

3 E. S. Choi, J. S. Brooks, D. L. Eaton, M. S. Al-Haik, M. Y. Hussaini, H. Garmestani, D. Li, K. Dahmen, J. Appl. Phys. 2003, **94**, 6034.

4 T. Kimura, H. Ago, M. Tobita, S. Ohshima, M. Kyotani, M. Yumura, Adv. Mater. 2002, **14**, 1380.

5 B. Polyak, I. Fishbein, M. Chorny, I. Alferiev, D. Williams, B. Yellen, G. Friedman, R. J. Levy, Proc. Natl. Acad. Sci. USA 2008, **105**, 698.